

ORIGINAL ARTICLE



Experimental Assessment of Stainless and Carbon Steel Double-Skin Tubular Stub Columns Filled with Recycled Aggregate Concrete

Deborah S. Castanheira^{1,2}, Luciano R. O. de Lima³, Pedro C. G. da S. Vellasco³, Katherine A. Cashell⁴ and Leroy Gardner²

Correspondence

Deborah S. Castanheira
PhD student
UERJ - State University of Rio de Janeiro
Rua São Francisco Xavier, 524, sala 5018A
Maracanã, Rio de Janeiro, RJ, Brazil
20550-900
Email: deborahcastanheira@gmail.com

Affiliations

¹ PGE CIV - Civil Engineering Post-Graduate Program, UERJ - State University of Rio de Janeiro, Brazil

² Department of Civil and Environmental Engineering, Imperial College London, London, UK

³ Structural Engineering Department, UERJ - State University of Rio de Janeiro, Brazil

⁴ Department of Civil and Environmental Engineering, Brunel University London, UK

Abstract

This paper presents an experimental study into the behaviour of concrete filled double skin tubular (CFDST) stub columns. A total of eight axial compression tests were carried out, half of which were filled with conventional concrete and the remainder had recycled aggregate concrete. The columns were circular in cross-section and comprised an austenitic stainless steel outer tube and a carbon steel inner tube, of varying dimensions. Accordingly, hollow ratios of 0.67 and 0.55 were considered. The recycled coarse aggregate was made by crushing test specimens from a previous research project. A replacement ratio of 50% was adopted in these tests. Both the natural coarse aggregates and the recycled aggregates had a maximum diameter of 9.5 mm. During the tests, similar structural behaviour and failure modes were observed between the columns with conventional and recycled aggregate concrete, and the failure modes were identical. The experimental results are compared with available design procedures and it is ultimately shown that using recycled aggregate concrete rather than regular concrete in CFDST stub columns does not have a significant effect on the performance.

Keywords

Composite columns, Double-skin columns, Stainless steel, Carbon steel, Circular tubes, Recycled aggregate concrete, Experimental analysis.

1 Introduction

Concrete-filled double-skin tubular (CFDST) columns comprise two steel tubes with different dimensions concentrically positioned one inside the other and concrete infill in the space between the tubes. This type of composite column can be formed from different cross-sectional shapes, including square, rectangular, circular or elliptical sections. CFDST members are employed in many types of structural applications, such as offshore platforms, bridge piers, high-rise buildings and transmission towers, and have been the subject of significant research interest in recent years (e.g. 1-7). Their advantages are very similar to those of concrete-filled tubular (CFT) columns, and include higher compressive load-carrying capacity, greater ductility, and improved fire resistance [7] compared with bare steel sections. In addition, CFDST columns can result in lighter structures with lower construction costs compared with other structural solutions like concrete-filled tubular (CFT) columns, due to the hollow inner core and the reduced requirements for expensive formwork.

The current paper is concerned with the behaviour of CFDST columns with circular stainless steel outer tubes, circular carbon steel

inner sections and recycled aggregate concrete (RAC) for the infill. Stainless steel is a popular material for structural engineering applications owing to its many attributes, including excellent corrosion resistance, high strength and ductility, low maintenance requirements, aesthetic appeal and environmental credentials in terms of being fully recyclable. The sustainability of construction materials is hugely topical and therefore the use of recycled aggregates in concrete is currently receiving significant attention from the research community. RAC is made from demolished concrete elements which would otherwise have been condemned to landfill and also removes the need for new aggregate materials to be sourced [8]. It is generally agreed that the recycled aggregates (RA) should ideally be derived only from crushed concrete, without any impurities in the composition [9], in order to maintain good mechanical performance. Concrete made from recycled aggregates tends to have lower strength and stiffness compared with natural coarse aggregate concrete (NAC) due to the manufacturing process and the likely presence of cement paste, which increases the porosity and therefore the levels of water absorption [10].

The design of CFDST columns is not currently covered by international design standards. However, a number of researchers have

studied their behaviour in recent years. Uenaka *et al.* experimentally investigated these columns with carbon steel for both the outer and the inner tubes and proposed an equation for the determination of their ultimate axial capacity [3]. Han *et al.* conducted more than 80 tests on CFDST columns, including members with stainless steel outer tubes and carbon steel inner tubes [11]. Various parameters were studied in this programme including different cross-sections, column types and hollow ratios χ (see equation 1). It was shown that in general, the ultimate axial capacity increases with a reduction in χ whereas the ductility reduces. An equation for calculating the load-carrying capacity of double skin columns with stainless steel outer tubes, considering the hollow ratio, was proposed and will be further examined later in this paper.

The influence of the inner tube material on the structural performance of circular CFDST columns has also been studied through experiments and finite element analysis [12]. In this research, the outer tubes were made from stainless steel whereas high strength steel was employed for the inner tubes. A range of different geometries was examined and it was shown that current design provisions are generally safe-sided but do not adequately account for strain hardening in the steel tubes, or the influence of concrete confinement, on the load-carrying capacity.

There have been a number of studies into the use of recycled aggregate concrete in composite elements in recent years [e.g. 13-16], including on CFT columns where there is a significant contribution made by the confined concrete to the overall performance [14]. It has been shown that as the replacement ratio of natural coarse aggregate with recycled aggregate increases, the ultimate load and stiffness of a composite column generally decreases [14]. Currently, there is a dearth of information available in the literature on CFDST stub columns made from a combination of stainless steel, carbon steel and recycled aggregate concrete. Accordingly, this paper presents an experimental study into this type of member. The details of the experimental programme are discussed and the results are compared with the guidance given in design codes and other available literature.

2 Experimental Programme

2.1 General

The experimental programme comprised eight tests on circular CFDST stub columns and was conducted in the Civil Engineering Laboratory at the State University of Rio de Janeiro (UERJ) in Brazil. All of the columns comprised an outer tube made from grade 1.4307 austenitic stainless steel and an inner tube in grade VMB300 hot-rolled carbon steel. The dimensions are given in Table 1, including the diameters of the outer D and inner d tubular sections as well as their respective thicknesses, t_{so} and t_{si} . Four of the samples (NAC1-NAC4) contained natural aggregate concrete (NAC) while the remaining four samples (RAC1-RAC4) were infilled with recycled aggregate concrete (RAC). By varying the diameter of the inner tube, two hollow ratios χ , equal to either 0.55 or 0.67, were considered. The hollow ratio is defined as:

$$\chi = d / (D - 2t_{so}) \quad (1)$$

This expression was introduced by Han *et al.* [11] and it was also suggested that the ideal range for the hollow ratio of CFDST circular stub columns is between 0.5 and 0.7. The stub column lengths were taken as approximately three times the outer tube diameter, in accordance with Han *et al.* [11], to ensure that global buckling failure did not occur. A typical cross-section is shown in Figure 1(a). Small steel bars with a diameter of 5.5 mm were welded to the inner steel tube as shown in Figure 1(b) to maintain concentricity during concrete casting.

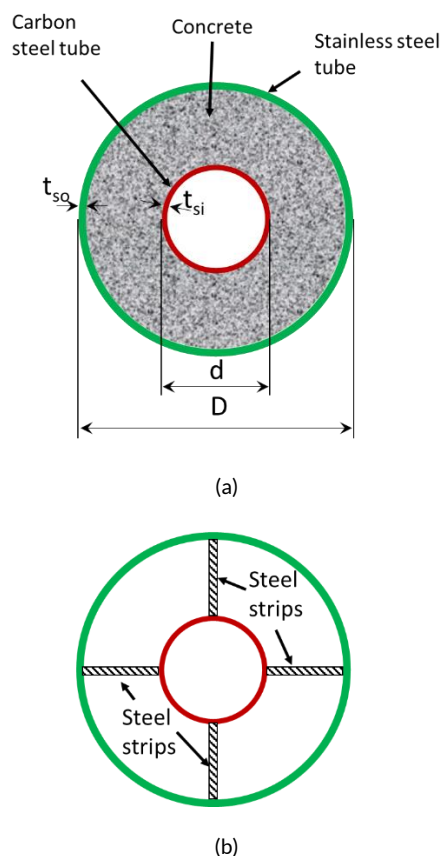


Figure 1 Schematic of the CFDST cross-sections (a) after casting and (b) showing the steel bars included to maintain concentricity

Table 1 Measured geometry and ultimate loads from the tested CFDST stub columns

Specimen	L (mm)	D (mm)	t_{so} (mm)	d (mm)	t_{si} (mm)	$N_{u,test}$ (kN)
NAC1	550.0	168.3	2.8	88.9	5.5	1941
NAC2						1865
NAC3				108.4	4.5	1649
NAC4						1612
RAC1	500.0			88.9	5.5	2087
RAC2						2075
RAC3				108.4	4.5	1682
RAC4						1693

2.2 Tubular sections

The mechanical properties of the carbon steel inner tubes were measured by the manufacturing company. A yield strength f_y of 375 N/mm², Young's modulus E of 200 kN/mm² and ultimate strength f_u of 474 N/mm² were reported. The mechanical properties of the austenitic stainless steel outer tubes were obtained through tensile coupon testing, which was conducted in accordance with EN 10002-1 [17] and the testing procedure for curved coupons given by Huang and Young [18]. The Young's modulus, 0.2% proof strength $f_{0.2}$, ultimate strength, and total elongation at fracture (measured over a 50 mm gauge length) ϵ_f were found to be 197 kN/mm², 419 N/mm², 674 N/mm² and 59 %, respectively. A typical stress-strain curve from the tensile tests on the stainless steel outer tube is depicted in Figure 2.

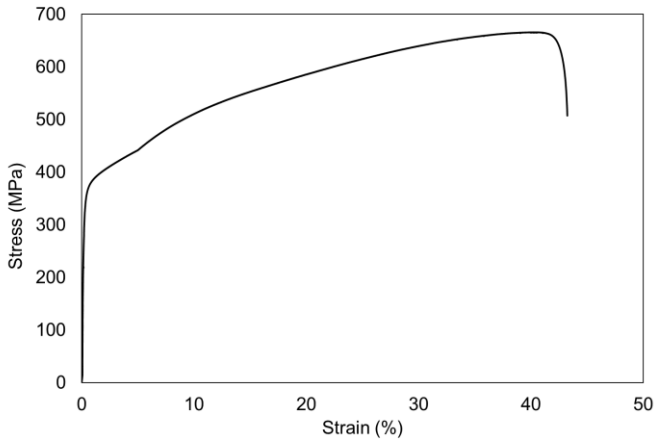


Figure 2 Typical stress-strain response for austenitic stainless steel used for the outer tubular section

2.3 Concrete

The test specimens were cast in two series using the same concrete mix design, which is presented in Table 2. The first series contained natural coarse aggregate (NA) whereas the second series had 50% of this replaced with the same amount of recycled coarse aggregate (RA). A superplasticiser was included in both mixes to make the concrete more workable, and the quantity was selected as 0.15% of the cement weight. The conventional concrete (NAC) and the RAC reached an average compressive cylinder strength f_c of 30 and 33 MPa, respectively. This was determined by conducting compressive tests on cylindrical samples that were cast from the same batch of concrete, on the same day that the corresponding columns were tested. This was 40 days after casting for the NAC columns and 30 days after casting for the RAC specimens.

Table 2 Details of the concrete mix design

Mix proportions (to weight of cement)	NAC	RAC
Cement	1.00	
Sand	2.29	
NA	1.58	0.79
RA	0	0.79
Water/cement ratio	0.43	0.46
Superplasticizer	0.0015	

The recycled aggregate was manufactured through the crushing of concrete elements from a previous experimental campaign [19], as shown in Figure 3, which had an average compressive cylinder strength of 41 MPa. The characteristic properties of the aggregates used in the concrete were determined prior to casting in accordance with the relevant Brazilian standards [20-22], and the data are given in Table 3. It is noteworthy that the recycled aggregates had a significantly greater water absorption capacity compared with the natural coarse aggregates. In accordance with the guidance of other researchers who have worked with RAC [e.g. 23, 24], the recycled aggregates were treated before casting by first sieving to ensure that the particles were the same size as the natural coarse aggregates and then adding water just before casting and mixing it in the saturated condition.

Table 3 Characteristics of the coarse aggregates

Property	NAC	RAC
Fineness modulus (%)	5.56	
Maximum diameter (mm)	9.50	
Bulk density (kg/m^3)	1370	1090
Pore volume (%)	49.59	59.60
Specific gravity (kg/m^3)	2710	2700
Water absorption (%)	1.38	11.91



Figure 3 View of the crushed concrete to make the RAC

2.4 Test setup

The tests were conducted using a 3000 kN displacement-controlled universal testing machine. The columns were placed concentrically in the machine, and an axial displacement was then applied. Two plates with a thickness of 32 mm were placed at either end of the columns. The bottom end of the columns had fixed boundary conditions. The top end had a ball seating that locked upon the application of load, hence also providing fixed boundary conditions. To avoid the "elephant foot" buckling mode, a circular ring made from high strength steel (HSS) was placed close to the column ends, as recommended by other researchers [12,25]. The instrumentation employed in the tests included four displacement transducers (LVDTs) and four axial strain gauges at the mid-height of the columns to obtain the lateral displacements and strains, and two further LVDTs at the bottom plate to measure the longitudinal displacement, as shown in the schematic presented in Figure 4.

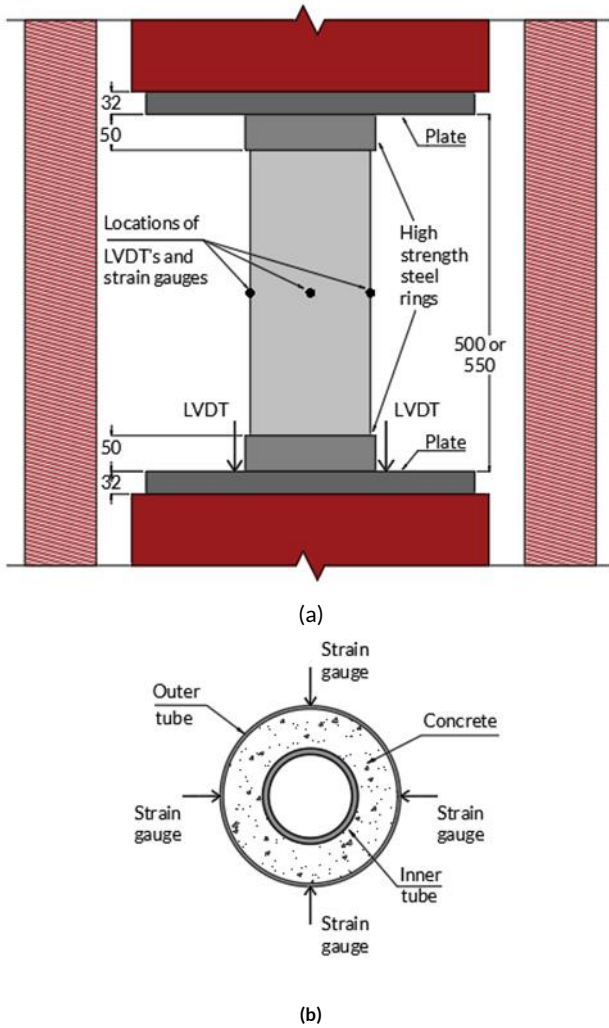


Figure 4 Schematic view of the test arrangement (all dimensions are in mm) in (a) elevation and (b) plan view

3 Test results

The compressive behaviour of the CFDST stub columns was observed during the tests and the peak loads ($N_{u, test}$) are presented in Table 1. It is clear that the columns with the smaller inner tubes and therefore larger volumes of concrete infill (i.e. NAC1, NAC2, RAC1 and RAC2) had greater ultimate load-carrying capacities compared with the columns with larger inner tubes and smaller concrete volumes (i.e. NAC3, NAC4, RAC3 and RAC4), as expected.

In terms of the aggregate type, the columns with RAC generally achieved higher load-carrying capacities than the equivalent members with NAC, reflecting the higher strength of the RAC concrete. Figure 5 presents images of two of the CFDST stub columns after testing, showing (a) outward-only local buckling of the outer tube, accompanied by the suggestion of shear failure in the concrete and (b) inward-only local buckling of the inner tube. The same failure mode was observed in all eight specimens. The presence of the infill concrete prevented the steel tubes from buckling locally in both directions.



(a)



(b)

Figure 5 Images of the specimens after testing showing (a) outward-only local buckling of the outer stainless steel tube of RAC3 and RAC4 and (b) inward-only local buckling of the inner carbon steel tube for RAC3

3.1 Axial load versus axial displacement

Figure 6 presents the experimental results in terms of axial load versus axial displacement for all of the CFDST stub column tests. The axial displacement value was measured by two LVDTs on the bottom plate, as previously discussed, and the average value is presented. Specimens NAC1, NAC2, RAC1 and RAC2 (i.e. those with the smaller inner steel tubes) are shown in Figure 6(a) and specimens NAC3, NAC4, RAC3 and RAC4 (i.e. those with the larger inner steel tubes) are shown in Figure 6(b). In both cases, it is observed that irrespective of the concrete type, all of the specimens behaved in a relatively similar manner. Initially, during the elastic range, the load-displacement behaviour was linear until the first peak occurred. For the RAC specimens, this was followed by a plateau in which the load remained constant for a period which was not observed in the NAC tests. This is likely to be due to some localised crushing of the concrete. Thereafter, the load continued to increase until an axial displacement of around 15–20 mm, after which the load began to drop as failure occurred.

It is noteworthy that the specimens in Figure 6(a), which had a greater volume of concrete and smaller inner tube, reached higher displacements at the peak load (around 22 mm) compared with the specimens in Figure 6(b) which reached a displacement of around 17 mm at the maximum load. Furthermore, for the specimens with

the lower volumes of concrete (Figure 6(b)), the CFDST columns with NAC were generally more ductile than those with RAC. This phenomenon was not so clear in the responses shown in Figure 6(a) for the columns with a smaller inner tube and therefore more concrete.

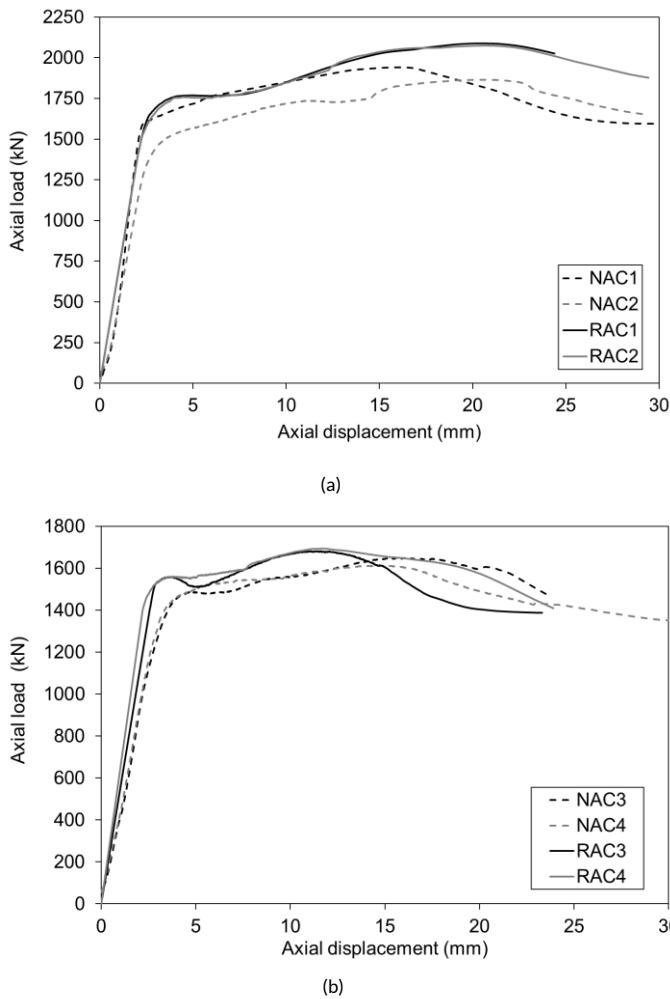


Figure 6 Axial load versus axial displacement curves for the CFDST columns with (a) smaller inner tubes and (b) larger inner tubes

3.2 Axial load versus average axial strain

Figure 7 presents the strain data in terms of axial load versus axial strain for (a) the specimens with smaller inner tubes and (b) those with larger inner tubes. As explained previously, four strain gauges were affixed to each column positioned in the four quadrants, at the mid-height location. The average longitudinal strains from the four measured values are illustrated in the graphs. Strains were measured up to about 2% strain. There was some variation in the initial stiffnesses of the specimens, with the NAC columns exhibiting generally a stiffer response, compared with their RAC counterparts.

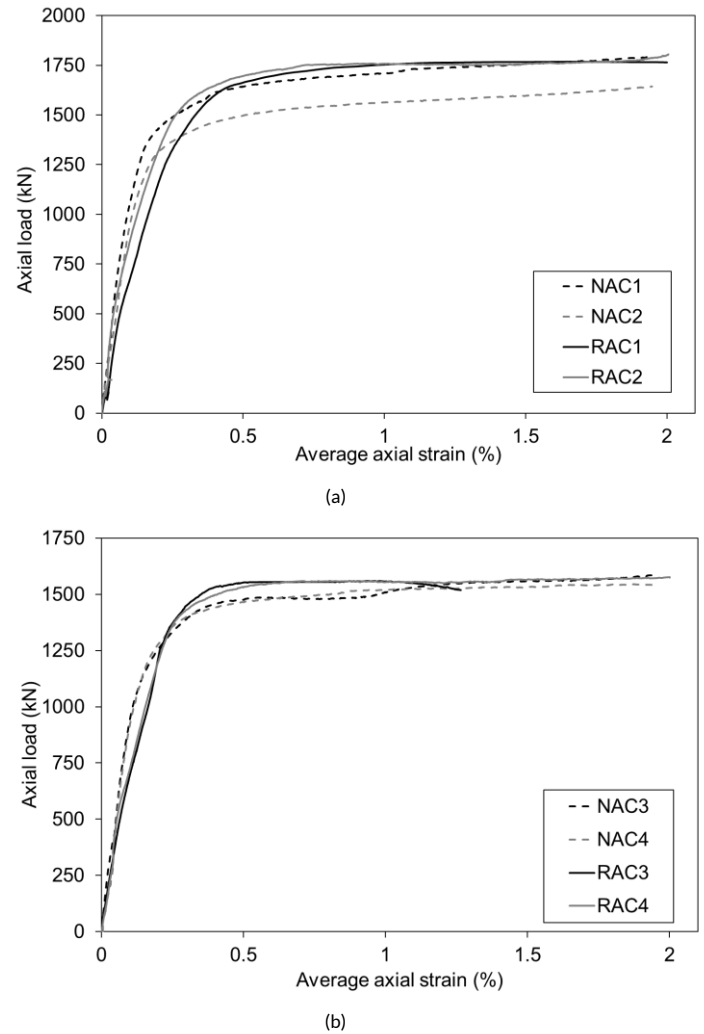


Figure 7 Axial load versus average axial strain for the CFDST columns with (a) smaller inner tubes and (b) larger inner tubes

4 Comparison with design expressions

The design of CFDST stub columns is not yet explicitly covered by international design standards. Nevertheless, existing design rules for concrete-filled tubes in Eurocode 4 [26] and the American specification AISC 360 [28] are assessed herein. The applicability of these design rules to CFDST sections is evaluated through comparisons of the experimental axial capacities with the code-predicted axial capacities. In addition, the procedure developed by Han *et al.* for the design of CFDST columns is examined [11].

The approach proposed by Han *et al.* [11] is based on the assumption that the ultimate strength of a CFDST stub column $N_{u,Han}$ is equal to the sum of the capacities of the inner tube $N_{i,u}$ and the outer tube and concrete combined $N_{osc,u}$, respectively, as given in equation 2:

$$N_{u,Han} = N_{i,u} + N_{osc,u} \quad (2)$$

The capacities of the two components in equation 2 are determined in accordance with equations 3 and 4, respectively:

$$N_{i,u} = A_{si} f_{syi} \quad (3)$$

$$N_{osc,u} = A_{soc} f_{osc} \quad (4)$$

in which f_{syi} is the yield strength of the inner tube and f_{osc} is a combined strength value for the outer stainless steel tube f_{syo} and the concrete infill f_c accounting for the confinement effect. In this case,

since the outer tube is made from stainless steel, the yield strength f_{syo} is taken as the 0.2% proof strength $f_{0.2}$. A_{si} is the cross-sectional area of the inner tube whilst A_{soc} is the sum of the cross-sectional areas of the outer stainless steel tube A_{so} and the concrete A_c :

$$A_{soc} = A_{so} + A_c \quad (5)$$

The combined strength value for the outer stainless steel tube and the infill concrete is given by equation 6:

$$f_{osc} = C_1 \chi^2 f_{syo} + C_2 (1.14 + 1.02\xi) f_c \quad (6)$$

In this expression, χ is the hollow ratio determined using equation 1, C_1 and C_2 are found using equations 7 and 8, respectively, and ξ is the nominal confinement factor, defined below.

$$C_1 = \alpha / (1 + \alpha) \quad (7)$$

$$C_2 = (1 + \alpha_n) / (1 + \alpha) \quad (8)$$

In these equations, α is the ratio of the area of the outer stainless steel tube A_{so} to the cross-sectional area of concrete A_c and α_n is the ratio of A_{so} to A_{ce} . A_{ce} is an equivalent cross-sectional area of the sandwiched concrete, defined as the full area enclosed by the outer tube, as given by equation 9:

$$A_{ce} = \pi(D - 2t_{so})^2 / 4 \quad (9)$$

The nominal confinement factor ξ is found from equation 10:

$$\xi = A_{so} f_{syo} / A_{ce} f_c \quad (10)$$

Eurocode 4 includes a design equation for the strength of concrete filled tubes (CFT), $N_{u,EC4}$, based on the summation of the capacities of the three component elements, i.e. the outer steel tube, the concrete infill and the reinforcement, if present [26], as given in equation 11:

$$N_{u,EC4} = A_{so} f_{syo} + A_c f_c + A_{sa} f_{sya} \quad (11)$$

In this expression, A_{sa} and f_{sya} are the cross-sectional area and yield strength of the internal reinforcement, or encased steel section, and can be replaced with A_{si} and f_{syi} in the current analysis. Wang *et al.* [27], proposed a modification to the Eurocode 4 design equation for CFDST columns to account for the contribution made to the capacity by the inner steel tube. In this, the contribution of the reinforcement, as included in equation 11, is replaced by the corresponding term for the inner steel tube.

The American ANSI/AISC design standard for composite columns

presents a design equation for the column strength which is very similar to the European code, and is based on a summation of the contributions of the outer steel tube, the concrete infill and the internal steel reinforcement to the overall capacity [28]. However, this code distinguishes between compact, non-compact and slender columns. In the equation for compact columns, as is relevant to the current work, the strength of the internal steel reinforcement is replaced by the inner steel tube cross-section, as given in equation 12, to give the strength of the section $N_{u,AISC}$ as:

$$N_{u,AISC} = A_{so} f_{syo} + 0.95 A_c f_c + A_{si} f_{syi} \quad (12)$$

Table 4 presents the experimental results for each of the eight CFDST columns previously discussed $N_{u,test}$, as well as the predicted ultimate load capacities determined using the method proposed by Han *et al.* [11] $N_{u,Han}$, Eurocode 4 [26] $N_{u,EC4}$ and AISC 360 [28] $N_{u,AISC}$.

The data in the table show that all three design methods assessed provide conservative predictions of the load-carrying capacity. Generally, the method proposed by Han *et al.*, [11] gives the most accurate and least scattered load-carrying capacity predictions, with an average test/predicted ratio of 1.08 and a coefficient of variation (COV) of 0.068. On the other hand, the Eurocode 4 [26] and AISC [28] methods provide more conservative estimations, with average test/predicted load ratios of 1.17 and 1.18, respectively. This is to be expected since the method proposed by Han *et al.* is the only that specifically considers the confinement afforded to the concrete in CFDST sections; the European and American design standards are for CFT sections.

It is also evident from the data presented in the table that the design methods provide more accurate strength predictions (i.e. within 3% [11], 10% [26] and 12% [28]) for the columns with the larger inner tubes (i.e. NAC3, NAC4, RAC3 and RAC4). On the other hand, for the columns with the smaller inner tubes and therefore the greater volumes of concrete infill, the design equations are less accurate, supporting the above suggestion that the conservatism is related primarily to the underprediction of the capacity of the concrete.

5 Conclusions

This paper presents the details and results from an experimental study into the behaviour of CFDST stub columns under concentric compressive loading. Eight stub columns were tested in two groups: the first with conventional concrete made from natural coarse aggregates (NAC) and the second with recycled coarse aggregate concrete (RAC). In all cases, the outer steel tube was made from grade 1.4307 cold-formed austenitic stainless steel and the inner tube was made from hot-rolled carbon steel. Two sizes of inner tube were considered to provide variation in the hollow ratio χ .

Table 4 Comparison of experimental results and design codes predictions.

Specimen	$N_{u,test}$ (kN)	$N_{u,Han}$ (kN)	$N_{u,EC4}$ (kN)	$N_{u,AISC}$ (kN)	$N_{u,test} / N_{u,Han}$	$N_{u,test} / N_{u,EC4}$	$N_{u,test} / N_{u,AISC}$
NAC1	1941	1718	1583	1561	1.13	1.23	1.24
NAC2	1865				1.09	1.18	1.19
RAC1	2087	1766	1622	1599	1.18	1.29	1.31
RAC2	2075				1.18	1.28	1.30
NAC3	1649	1609	1503	1485	1.02	1.10	1.11
NAC4	1612				1.00	1.07	1.09
RAC3	1682	1647	1534	1515	1.02	1.10	1.11
RAC4	1693				1.03	1.10	1.12
Average					1.08	1.17	1.18
COV					0.068	0.075	0.076

The failure mode, ultimate load and ductility of each specimen has been presented and discussed, and then compared with available design expressions. It was shown that, as expected, a higher ultimate capacity was achieved by the columns with a relatively larger concrete area. The proposed design equation from Han *et al.* [11] provides excellent agreement with the test data. On the other hand, the design expressions for composite columns given in the European and American design standards are shown to provide rather conservative capacity predictions. Of course, these expressions were developed for concrete filled tubular columns rather than concrete filled double skin tubular members.

One of the main aims of this work was to examine the performance of CFDST stub columns with recycled aggregate concrete (RAC), relative to regular concrete with natural coarse aggregate. In this context, the tests showed that the NAC and the RAC behaved in a very similar manner and achieved comparable ultimate load-carrying capacities.

References

- [1] S. Wei, S. T. Mau, C. Vipulanandan, S. K. Mantrala. Performance of New Sandwich Tube Under Axial Loading: Experiment, *Journal of Structural Engineering*. 121(12) (1995) 1806-1814.
- [2] X-L. Zhao, R. Grzebieta, M. Elchalakani. Tests of concrete-filled double skin CHS composite stub columns, *Steel and Composite Structures*. 2(2) (2002) 129-146.
- [3] K. Uenaka, H. Kitoh, K. Sonoda. Concrete filled double skin circular stub columns under compression, *Thin-Walled Structures*. 48 (2010) 19-24.
- [4] W. Li, L-H. Han, X-L. Zhao. Axial strength of concrete-filled double skin steel tubular (CFDST) columns with preload on steel tubes, *Thin-Walled Structures*. 56 (2012) 9-20.
- [5] L-H. Han, W. Li, R. Bjorhovde. Developments and advanced applications of concrete-filled steel tubular (CFST) structures: Members, *Journal of Constructional Steel Research*. 100 (2014) 211-228.
- [6] Z. Tao, L-H. Han, X-L. Zhao. Behaviour of concrete-filled double skin (CHS inner and CHS outer) steel tubular stub columns and beam-columns, *Journal of Constructional Steel Research*. 60 (2004) 1129-1158.
- [7] H. Lu, L-H. Han, X-L. Zhao. Fire performance of self-consolidation concrete filled double skin steel tubular columns: Experiments, *Fire Safety Journal*. 45 (2010) 106-115.
- [8] A. E. B. Cabral, V. Schalch, D. C. C. Dal Molin, J. L. D. Ribeiro. Mechanical properties modelling of recycled aggregate concrete, *Construction and Building Materials*. 24 (2010) 421-430.
- [9] M. J. McGinnis, M. Davis, A. de la Rosa, B. D. Weldon, Y. C. Kurama. Strength and stiffness of concrete with recycled concrete aggregates, *Construction and Building Materials*. 154 (2017) 258-269.
- [10] R. V. Silva, J. de Brito, R. K. Dhir. Properties and composition of recycled aggregates from construction and demolition waste suitable for concrete production, *Construction and Building Materials*. 65 (2014) 201-217.
- [11] L-H. Han, Q-X. Ren, W. Li. Tests on stub stainless steel-concrete-carbon steel double-skin tubular (DST) columns, *Journal of Constructional Steel Research*. 67 (2011) 437-452.
- [12] F. Wang, B. Young, L. Gardner. Compressive testing and numerical modelling of concrete-filled double skin CHS with austenitic stainless steel outer tubes, *Thin-Walled Structures*. 141 (2019) 345-359.
- [13] Y. Huang, J. Xiao, X. Huang. Properties of Confined Recycled Aggregate Concrete, 2nd International Conference on Waste Engineering and Management. 1 (2010) 743-755.
- [14] Z. Chen, J. Xu, J. Xue, Y. Su. Performance and Calculations of Recycled Aggregate Concrete-filled Steel Tubular (RACFST) Short Columns under Axial Compression, *International Journal of Steel Structures*. 14 (2014) 31-42.
- [15] J. Xiao, Y. Huang, J. Yang, C. Zhang. Mechanical properties of confined recycled aggregate concrete under axial compression, *Construction and Building Materials*. 26 (2012) 591-603.
- [16] Y. Huang, J. Xiao, C. Zhang. Theoretical study on mechanical behaviour of steel confined recycled aggregate concrete, *Journal of Constructional Steel Research*. 76 (2012) 100-111.
- [17] EN 10002-1: 1990. Metallic materials – Tensile testing – Part 1: Method of test at ambient temperature. CEN, European Committee for Standardization, Brussels.
- [18] Y. Huang, B. Young. The art of coupon test, *Journal of Constructional Steel Research*. 96 (2014) 159-175.
- [19] B.N.T. De Macedo. Determinação do coeficiente de conformação superficial de barras de aço para uso em concreto armado, MSc Dissertation, PGECIV – Post Graduate Program in Civil Engineering, State University of Rio de Janeiro – UERJ, 2018 (in Portuguese).
- [20] ABNT NBR 7251 (1982) Agregados em estado solto – Determinação da massa unitária – Método de ensaio, Associação Brasileira de Normas Técnicas, Rio de Janeiro, Brazil (in Portuguese).
- [21] ABNT NBR NM 45 (2006) Agregados – Determinação da massa unitária e do volume de vazios, Associação Brasileira de Normas Técnicas, Rio de Janeiro, Brazil (in Portuguese).
- [22] ABNT NBR NM 52 (2002) Agregado miúdo – Determinação de massa específica e massa específica aparente, Associação Brasileira de Normas Técnicas, Rio de Janeiro, Brazil (in Portuguese).
- [23] V. W. Y. Tam, C. M. Tam. Parameters for assessing recycled aggregate and their correlation, *Waste Management & Research*. 27 (2009) 52-58.
- [24] R. V. Silva, J. de Brito, R. K. Dhir. The influence of the use of recycled aggregates on the compressive strength of concrete: a review, *European Journal of Environmental and Civil Engineering*. 19 (2015) 825-849.
- [25] X. Meng, L. Gardner. Cross-sectional behaviour of cold-formed high strength steel circular hollow sections.

Submitted to Thin-Walled Structures. 2020.

- [26] Eurocode 4, EN 1994-1-1: 2004. Design of Composite Steel and Concrete Structures, Part 1.1: General Rules and Rules for Buildings. CEN, European Committee for Standardization, Brussels.
- [27] F. Wang, B. Young, L. Gardner. Wang, F. CFDST sections with square stainless steel outer tubes under axial compression: Experimental investigation, numerical modelling and design. Engineering Structures. 207(2020), 110189.
- [28] ANSI/AISC 360-10. Specification for Structural Steel Buildings, American Institute of Steel Construction, 2010, Chicago, Illinois, USA.